

Research Article

Nickel Transmutation and Excess Heat Model using Reversible Thermodynamics

Daniel S Szumski*

Independent Scholar, 513F Street, Davis, CA 95616, USA

Abstract

This research develops the Least Action Nuclear Process (LANP) model of cold fusion, by assuming that the process is thermodynamically reversible. This requires: (1) one element of new physical theory, a far-from-equilibrium black body equation having a second temperature scale and (2) a nuclear reaction selection method based on the Principle of Least Action. The model appears to predict nuclear transmutations observed in Miley's nickel microspheres, without false positives, and provides a plausible explanation of loading and ignition processes, excess heat, no excess heat, and the absence of gamma radiation. The model shows how solar core temperatures can exist in a laboratory temperature device. This presentation is abstracted from a larger technical paper.

© 2014 ISCMNS. All rights reserved. ISSN 2227-3123

Keywords: LANP model, Least action, Reversible process, Theory

1. Introduction

During the last two decades it has become evident that low energy nuclear reactions are occurring in Fleischmann–Pons (F–P) electrolytic cells [1]. These reactions are unprecedented in nuclear physics, and are at least for now, hidden from understanding because a suitable theoretical framework has not been forthcoming [2]. The degree to which new physics underlies these experimental observations is not known. But, among theoreticians it is considered more likely that the present conundrum will be resolved by extensions of known physical principles.

This research endeavors to provide insight into three theoretical issues. First, it explores a mechanism for accumulating the ignition energy. Second, it explores how this energy might be stored until the moment of ignition. And third, it proposes how the accumulated energy partitions to specific nuclear transformations, and not others. The goal here is to show how a different view of heat processes, one that includes both irreversible and reversible thermodynamics, might inspire a comprehensive cold fusion theory.

*E-mail: Danszumski@sbcglobal.net

2. Theory of Heat

Heat exists in two domains that continually exchange energy as any arbitrary thermal system tends toward new quasi-equilibrium states. These are the domain of molecular motion, and the domain of heat radiation. The first might be referred to as the *mass domain*. It was Helmholtz who first showed that molecular motion is equivalent to heat; an observation that is central to what follows.

Heat energy also exists in the *radiation domain*. The theoretical framework describing equilibrium conditions there bears the revered names of Rayleigh, Wien, and Planck. Planck's equation [3] describes the equilibrium temperature dependence of black body spectral emittance.

Reversible thermodynamic processes are believed to be rare in nature. These are processes that produce a net zero free energy change, and are described by the thermodynamic treatment of Helmholtz, but not that of Gibbs. In all cases, reversible processes can be completely described by the Principle of Least Action [4].

I have proposed [5] a mathematical form for the black body spectral distribution that permits a glimpse into its non-equilibrium, and far-from-equilibrium characteristics.

$$K(\nu_1) = \frac{\varepsilon_\nu}{a_\nu} = k_b T_m \frac{\nu_1^2}{c^2} \frac{1}{e^{f_3(\nu_1/\nu_m)}}, \quad (1)$$

Black body spectra = Emittance (Rayleigh Law)/Absorptance (Ref. [5]),

where

$$f_3(\nu_1/\nu_m) = \left(\frac{\nu_1}{\nu_m}\right)^2 \left[\frac{1}{2} \left(\ln \left(\frac{\nu_1}{\nu_m} \right) \right)^2 - \frac{3}{2} \ln \left(\frac{\nu_1}{\nu_m} \right) + \frac{7}{4} \right] \quad (2)$$

and

$$\nu_m = 5.89 \times 10^{10} T_R \text{ (K)} \quad \text{(Wein frequency)}, \quad (3)$$

where T_m is the thermodynamic temperature, T_R is a new quantity called the radiation temperature, and $K(\nu_1)$ exists where the number of quanta is equal to or greater than 1.

Planck's equilibrium equation is given by:

$$K(\nu_1) = h \nu_1 \frac{1}{c^2} \frac{1}{e^{h\nu/k_b T - 1}}. \quad (4)$$

The non-equilibrium form in Eq. (1) is close to, but not exactly, Planck's at equilibrium.

This theory suggests that independent temperature scales might represent the mass and radiation domains. Figure 1 illustrates characteristics of the far-from-equilibrium, black body radiation spectra.

Curve A, refers to the transient initial condition where heating is initiated by increasing molecular motion, for example, by frictional input of heat.

If an identical amount of heat is initially added to the radiation domain alone (i.e. higher energy radiation), T_m , is initially constant, and the Wein frequency increase shifts the emittance spectra to higher frequencies (curve B). Both of these cases decay to equilibrium spectra similar to, but with higher total energy than the initial equilibrium case. At the new equilibrium condition, the mass and radiation temperatures become identical, and it is not possible to determine from which of the two domains the original heating took place. However, as will be shown in what follows, there are circumstances under which the second of these spectra might be held in a far-from-equilibrium state, and in this way store vast amounts of energy in a nickel or palladium cathode that is apparently at about 60°C.

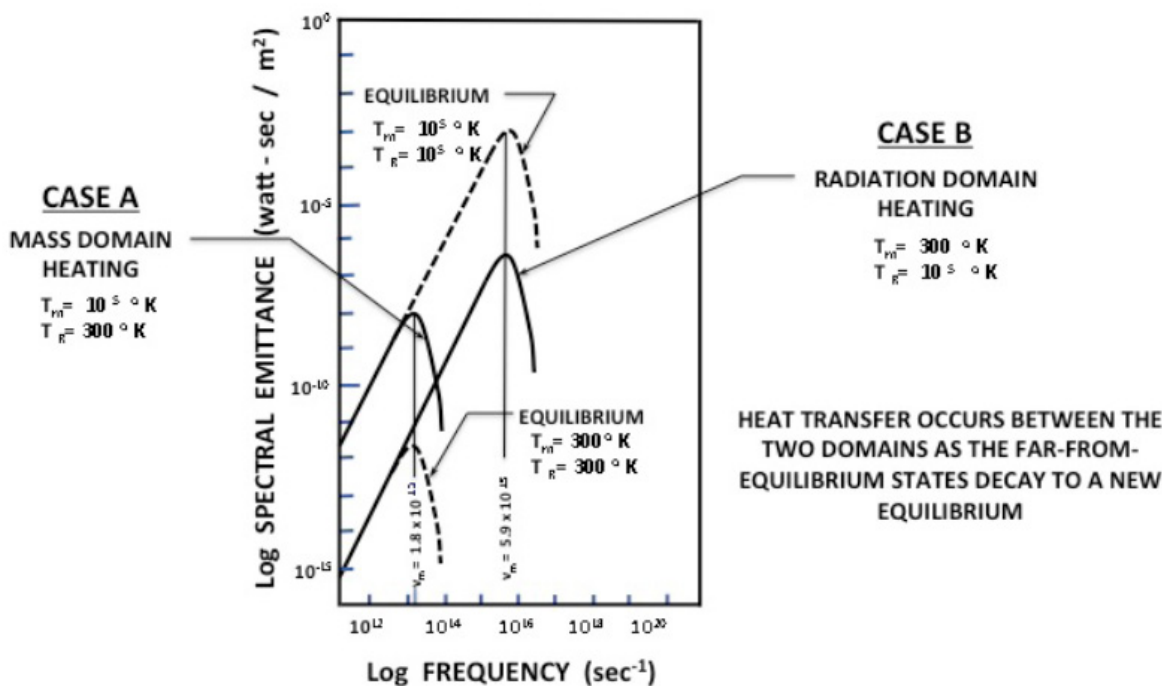


Figure 1. Illustration of non-equilibrium changes in the heat radiation spectra (Eq. (1)). Case A represents instantaneous mass domain heating (i.e. friction) at constant radiation temperature. Case B represents adiabatic heat accumulation at a constant thermodynamic temperature.

3. Consider a Thermodynamically Reversible Process

In thermodynamically reversible processes, be they chemical or nuclear, all of the process energy must be in a usable form. Thermal motion is specifically excluded, or it must be quieted; i.e. converted to radiation domain energy, as it enters the reaction space. In our case, a deuteron's kinetic energy is captured ('quieted') as it is absorbed from the heavy water into the metal lattice, adding to the internal lattice energy, and more specifically storing that captured kinetic energy in excited electron and excited nuclear states.

To place an order of magnitude estimate on this energy storage, we will use the 0.2 cm diameter \times 10 cm Pd electrode from Fleischmann and Pons 1989 experiments [1]. The surface area of the cathode is $6.28 \times 10^{-4} \text{ m}^2$. Assuming α -phase absorption approximating β -Pd D_{0.85}, and having a lattice parameter of 0.405 nm, the number of filled sites at the surface of the cathode, is approximated as 3.26×10^{15} sites in a single atomic layer at the cathode surface. If we assume that the average deuteron velocity is 0.2 m/s, the average kinetic energy of the deuterons in the cell can be calculated as $6.68 \times 10^{-22} \text{ erg}$, or a total of $2.2 \times 10^{-6} \text{ erg} = 1.35 \text{ MeV}$ in a single surface atomic layer. Thus, deuterium's 'quieted' thermal motion is more than sufficient for ignition. Where the electrode is being loaded in a deuterium gas environment the average molecular energy is $\frac{3}{2} k_b T$ at, or $6.89 \times 10^{-14} \text{ erg}$.

The loading energetics for metal hydrides are well understood [6–8] and the research reported here takes no issue with the known thermodynamics. Nevertheless, this theory is alone in associating the cold fusion ignition and process

Table 1. Selected nuclear reactions in Miley's nickel coated microspheres

Nuclear reaction	Initial isotope	Stable isotope	Energy change (amu)
$^{58}_{28}\text{Ni} + (6) \text{ }^2_1\text{H} \xrightarrow{\text{fusion}}$	$^{70}_{34}\text{Se}$	$^{70}_{32}\text{Ge}$ absent	-0.095706
$^{70}_{32}\text{Ge} \xrightarrow{\text{fission}}$		$(2) \text{ }^{35}_{16}\text{S} \xrightarrow{\beta^-} (2) \text{ }^{35}_{17}\text{Cl} \uparrow$	-0.082248
$^{62}_{28}\text{Ni} + (1) \text{ }^2_1\text{H} \xrightarrow{\text{fusion}}$	$^{64}_{29}\text{Cu}$	$^{64}_{28}\text{Ni}$	-0.014480
		$^{64}_{30}\text{Zn}$ absent (note 1)	-0.013304
$^{64}_{30}\text{Zn} \xrightarrow{\beta^+ \beta^+}$		$^{64}_{28}\text{Ni}$	-0.014480
$^{64}_{30}\text{Zn} \xrightarrow{\text{fission}}$	$(2) \text{ }^{32}_{15}\text{P}$		+0.005368
$(2) \text{ }^{32}_{15}\text{P} \xrightarrow{\beta^-}$		$(2) \text{ }^{32}_{16}\text{S}$	+0.001696
$(2) \text{ }^{32}_{16}\text{S} \xrightarrow{\text{fission}}$		$(4) \text{ }^{16}_8\text{O}$ Example	+0.037212
$^{58}_{28}\text{Ni} - (2) \text{ }^4_2\text{He} \xrightarrow{\alpha}$	$^{50}_{24}\text{Cr} \xrightarrow{\beta^+ \beta^+}$ (Note 2)	$^{50}_{22}\text{Ti}$	+0.014654
$^{58}_{28}\text{Ni} \xrightarrow{\text{fission}}$	$(2) \text{ }^{29}_{14}\text{Si}$		+0.0176465
$(2) \text{ }^{58}_{28}\text{Ni} \xrightarrow{\text{fusion}}$	$^{116}_{56}\text{Ba}$	$^{111}_{48}\text{Cd}, ^{112}_{50}\text{Sn}, ^{114}_{50}\text{Sn},$ $^{115}_{50}\text{Sn}, [^{116}_{50}\text{Sn}] \text{ abs}$	-0.0310552
$^{116}_{50}\text{Sn} \xrightarrow{\text{fission}}$		$(2) \text{ }^{58}_{26}\text{Fe}$	-0.0020673
$(2) \text{ }^{60}_{28}\text{Ni} \xrightarrow{\text{fusion}}$	$^{120}_{56}\text{Ba}$	$^{116}_{50}\text{Sn}, ^{118}_{50}\text{Sn}, [^{120}_{51}\text{Te}] \text{ absent}$	+0.0424482
$^{120}_{51}\text{Te} \xrightarrow{\text{fission}}$		$(2) \text{ }^{60}_{28}\text{Ni}$	0.0000000
$(2) \text{ }^{58}_{28}\text{Ni} + \text{ }^2_1\text{H}^+ \xrightarrow{\text{fusion}}$	$^{118}_{57}\text{La}$	$^{114}_{50}\text{Sn}, ^{116}_{50}\text{Sn}, ^{117}_{50}\text{Sn}, [^{118}_{50}\text{Sn}]$	+0.016815
$(2) \text{ }^{60}_{28}\text{Ni} + \text{ }^2_1\text{H}^+ \xrightarrow{\text{fusion}}$	$^{122}_{57}\text{La}$	$^{118}_{50}\text{Sn}, ^{121}_{51}\text{Sb}, [^{122}_{52}\text{Te}] \text{ absent (note 3)}$	+0.027369
$^{122}_{52}\text{Te} \xrightarrow{\text{fission}}$		$(2) \text{ }^{61}_{28}\text{Ni}$	+0.013562
$(2) \text{ }^{58}_{28}\text{Ni} + (3) \text{ }^2_1\text{H}^+ \xrightarrow{\text{fusion}}$	$^{122}_{59}\text{Pr}$	$^{118}_{50}\text{Sn}, ^{120}_{52}\text{Te}, ^{121}_{51}\text{Sb}, [^{122}_{52}\text{Te}] \text{ absent}$	-0.0099461

$^{122}_{52}\text{Te} \xrightarrow{\text{fission}}$		$(2) \text{ }^{61}_{28}\text{Ni}$	-0.050878
$^{122}_{52}\text{Te} \xrightarrow{\alpha} {}^4_2\text{He}$		$^{118}_{50}\text{Sn}$	+0.001162
$(2) \text{ }^{60}_{28}\text{Ni} + (3) \text{ }^2_1\text{H}^+ \xrightarrow{\text{fusion}}$	$^{126}_{59}\text{Pr}$	$^{125}_{52}\text{Te}, [^{126}_{54}\text{Xe} \uparrow]$	0.0003958
$^{60}_{28}\text{Ni} + {}^{61}_{28}\text{Ni} - {}^4_2\text{He} \xrightarrow{\text{fusion}}$	$^{117}_{54}\text{Xe}$	$^{116}_{50}\text{Sn}, [^{117}_{50}\text{Sn}]$	+0.015139
$^{58}_{28}\text{Ni} + {}^{60}_{28}\text{Ni} - (2) \text{ }^4_2\text{He} \xrightarrow{\text{fusion}}$	$^{110}_{52}\text{Te}$	$^{109}_{47}\text{Ag}, [^{110}_{48}\text{Cd}]$ absent	+0.042079
$^{110}_{48}\text{Cd} \xrightarrow{\text{fission}}$		$[(2) \text{ }^{55}_{24}\text{Mn}]$	+0.015167
$^{58}_{28}\text{Ni} + {}^{61}_{28}\text{Ni} - (2) \text{ }^4_2\text{He} \xrightarrow{\text{fusion}}$	$^{111}_{52}\text{Te}$	$^{110}_{48}\text{Cd}, [^{111}_{48}\text{Cd}]$	+0.042985
$^{58}_{28}\text{Ni} + {}^{62}_{28}\text{Ni} - (2) \text{ }^4_2\text{He} \xrightarrow{\text{fusion}}$	$^{112}_{52}\text{Te}$	$[^{112}_{50}\text{Sn}]$	+0.046336
$^{112}_{50}\text{Sn} \xrightarrow{\text{fission}}$		$[(2) \text{ }^{56}_{26}\text{Fe}]$ (note 4)	+0.019328
$^{58}_{28}\text{Ni} + {}^{64}_{28}\text{Ni} - (2) \text{ }^4_2\text{He} \xrightarrow{\text{fusion}}$	$^{114}_{52}\text{Te}$	$[^{114}_{50}\text{Sn}]$	+0.044676
$^{114}_{50}\text{Sn} \xrightarrow{\text{fission}}$		$[(2) \text{ }^{57}_{26}\text{Fe}]$	+0.012685
$(3) \text{ }^{64}_{28}\text{Ni} \xrightarrow{\text{fusion}}$	$^{192}_{84}\text{Po}$	$^{176}_{72}\text{Hf}, ^{184}_{76}\text{Os}, ^{188}_{76}\text{Os}, [^{192}_{78}\text{Pt}]$	+0.207437
$^{192}_{84}\text{Po} \xrightarrow{\text{fission}}$	$(2) \text{ }^{96}_{39}\text{Y}$	$(2) [^{96}_{40}\text{Zr}]$	+0.032648
$^{58}_{28}\text{Ni} + ^{107}_{47}\text{Ag} + {}^2_1\text{H}^+ \xrightarrow{\text{fusion}}$	$^{167}_{76}\text{Os}$	$^{143}_{60}\text{Nd}, ^{147}_{62}\text{Sm}, [^{155}_{64}\text{Gd}],$ $^{159}_{65}\text{Tb}, ^{163}_{66}\text{Dy}, [^{167}_{68}\text{Er}]$	+0.0775065
$^{167}_{68}\text{Er} \xrightarrow{\alpha}$		$^{163}_{66}\text{Dy}$	+0.0767937

${}^{61}_{28}\text{Ni} + {}^{107}_{47}\text{Ag} + (2) {}^2_1\text{H}^+ \xrightarrow{\text{fusion}}$	${}^{172}_{77}\text{Ir}$	${}^{164}_{68}\text{Er}, {}^{168}_{70}\text{Yb}, [{}^{172}_{70}\text{Yb}]$	+0.0720249
${}^{61}_{28}\text{Ni} + {}^{107}_{47}\text{Ag} + (2) {}^2_1\text{H}^+ \xrightarrow{\text{fusion}}$	${}^{114}_{55}\text{Cs}$	${}^{106}_{48}\text{Cd}, {}^{107}_{47}\text{Ag}, {}^{108}_{48}\text{Cd}, {}^{109}_{47}\text{Ag}, {}^{110}_{48}\text{Cd},$ ${}^{111}_{48}\text{Cd}, {}^{112}_{50}\text{Sn}, {}^{113}_{49}\text{In}, {}^{114}_{50}\text{Sn}$	
${}^{114}_{50}\text{Sn} - {}^4_2\text{He} \xrightarrow{\alpha}$		${}^{110}_{48}\text{Cd}$	-3.95358
${}^{112}_{50}\text{Sn} \xrightarrow{\beta^+\beta^+}$		${}^{112}_{48}\text{Cd}$	-1.951766
${}^{113}_{49}\text{In} - {}^4_2\text{He} \xrightarrow{\alpha}$		${}^{109}_{47}\text{Ag}$	-4.951832
${}^{114}_{50}\text{Sn} \xrightarrow{\text{fission}}$ (Note 3)		$[(2) {}^{57}_{26}\text{Fe}]$	-0.014203

Note 1: Believed to undergo $\beta^+\beta^+$ decay to ${}^{64}_{24}\text{Ni}$ with half-life of over 2.3×10^{18} years.

Note 2: Suspected of $\beta^+\beta^+$ decay to ${}^{50}_{22}\text{Ti}$ with half-life of not less than 1.3×10^{18} years.

Note 3: Theoretically capable of spontaneous fission.

Note 4: Lowest mass/nucleon of all nucleides. End product of Stellar nucleosynthesis.

Table notes were taken from “Isotopes of Elements”, Wikipedia, http://en.Wikipedia.org/wiki:Main_page,4/13/12

energy with the loading process. All other theoretical constructs take the matrix loading as a given, and then look for the ignition energy within the metal hydride matrix.

Hydrogen storage within the lattice structure is known to occur in distinct thermodynamic phases: α , $\alpha + \beta$, β . These are known to be thermodynamically reversible [6]. Let us now look at that next step.

How is this energy stored during the loading phase of the experiment? We will begin by assuming that deuterium loading is a singular, multi-site, reversible process. During loading, no energy is lost to thermal motion. Thus, the stored energy is either entirely in the radiation domain, or it moves to another energy type where it can be held in a completely reversible state. We will partition this energy storage into two components. The first is the mechanical work involved in expanding the metal lattice by up to 15% to accommodate high deuterium loadings. This is an adiabatic volume expansion, and thus, a reversible process. The second is the adiabatic storage of radiation domain energy to achieve ignition energies.

It appears to me that the best explanation for the lower bound for energy storage is within discrete covalent bonds; each covalent electron pair alternately absorbing and emitting electro-magnetic energy that remains in a wholly reversible state. As the total energy storage increases further, excited nuclear states become active bringing the reversibly stored cathode energy to gamma levels, where Mössbauer resonance, a reversible process, prevails, and energy storage occurs as resonant gamma exchange. This energy is stored entirely within the atomic structure of the lattice, and without any external manifestation. It is masked from observation.

In order to inquire about temperatures achieved in this reversible energy storage, we note that temperature is a derivative [4, p. 105], dQ/dt , measuring the emittance from any closed volume contained completely within the nickel electrode's interior, and where the Joules/s crossing the surface area of that volume completely describes its temperature. If our free body volume is around one of the electrons participating in covalent bond resonant energy

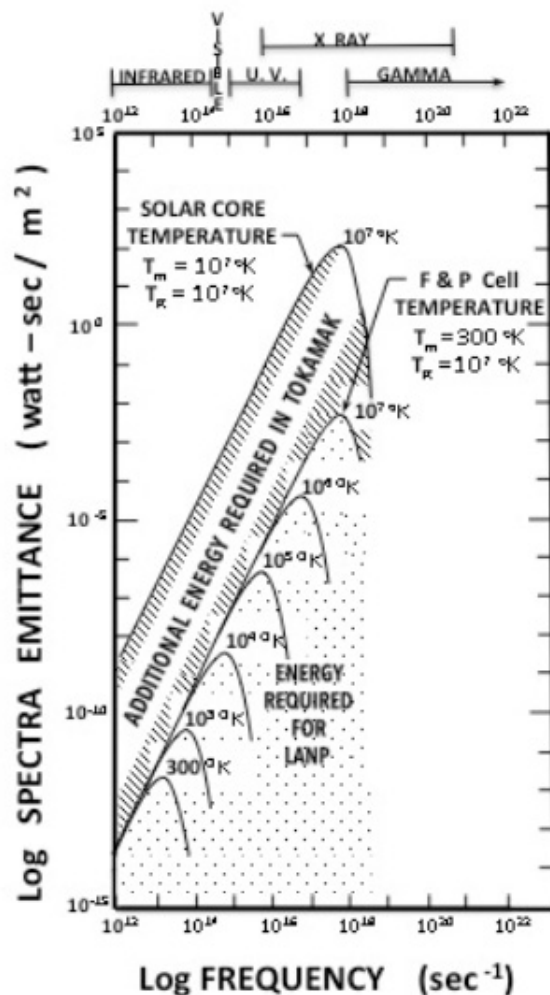


Figure 2. Comparison of theoretical radiation temperature structure in the F&P electrode with the solar core temperature. Both exhibit 10^7 K radiation temperature, but very different thermodynamic temperatures.

storage, the temperature is above the ambient thermodynamic temperature, T_m , but relatively small. However, as the frequency of the shared photon approaches gamma energies, the exchange takes place between nuclei, and the heat derivative, and thus the temperature within the volume containing one of these nuclei can become enormous, approaching and exceeding solar core temperatures.

The spectra labeled B in Fig. 1 represents the distribution of energy levels corresponding to this storage of heat energy. Eventually, the Wein frequency reaches gamma intensities, and the radiation temperature approximates that in the solar core, about 10^7 K as illustrated in Fig. 2. The figure contrasts the temperature regime (T_m and T_R) that this theory postulates to that in the solar core. It suggests that the energy spectra required for ignition in the Tokamak is about four orders of magnitude higher than that operative in the F&P cell, and much larger on a total energy basis. In essence,

the cold fusion process takes an energy shortcut around the enormous kinetic energy required for thermonuclear fusion. In this way, we see that the LANP is actually quite hot.

But, where are the Gamma emissions? We need to recall that we are dealing here with an extension of black body theory wherein electromagnetic energy of all wavelengths is emitted and absorbed within the lattice. The mass quantities involved in this absorption and emission are presumed to be electrons at the low energy end of the spectrum, and atomic nuclei as the energies increase through gamma intensities. Mass changes from any overall reaction occur as gamma emissions into the black body spectral distribution. Gamma emission and absorption are intrinsic to this system, internal to it, and in effect masked by it.

4. Experimental

Let us return to the mechanism of thermo-nuclear fusion/fission under these conditions. Miley's data from electrolysis of nickel coated microspheres [9] provides a suitable data set for analysis. I have inventoried what I believed are the most likely nuclear reactions occurring in the nickel coated microspheres. A small sampling of the 210 reactions (column 1) analyzed during this research is presented in Table 1. Isotope data are extracted from Wikipedia [10]. The second and third columns are the initial isotope formed, and the final stable product(s) of its decay. The last column is the total mass change in the nuclear reaction sequence that ends with the isotope in column 3.

Overall the data analysis shows that the reactions producing the lower atomic weight portion of the final electrode composition are: (1) fusion reactions of initial electrode isotopes (including impurities) with one or more deuterons, (2) fission reactions of initial electrode isotopes or isotopes that were *absent* from Miley's table, or (3) alpha decay. Some of the higher atomic weight isotopes result from fusion reactions involving nickel–nickel and nickel–impurities with deuterium nuclei. Because the initial electrode is severely neutron deficient relative to the final electrode, many of the high nuclear weight products probably have their origin in more complex stellar nucleosynthesis reactions. One thing that is clear is that neutron production is fundamental to the underlying nuclear process.

Many of these nuclear reactions have multiple isotope end points, and many of those are not in Miley's Table 3 [9]. I have identified one rule that determine which of these multiple isotope products will occur.

Rule 1: All fusion and fission reactions that can occur, are candidates. The one that actually produces a product along any reaction pathway is the reaction sequence that satisfies the Principle of Least Action (smallest overall mass change).

For each reaction shown, the isotope product that satisfies this condition is in **bold** type. Consider the nuclear reaction involving Miley's nickel electrode and one of its impurities : $^{58}_{28}\text{Ni} + ^{107}_{47}\text{Ag} + ^2_1\text{H}^+ \xrightarrow{\text{fusion}}$. It normally produces 38 intermediate radioactive isotopes and seven stable isotope products, three of which are in Miley's Table 3: $^{151}_{63}\text{Eu}$, $^{155}_{64}\text{Gd}$ and $^{163}_{66}\text{Dy}$. The results obtained from this reaction sequence are shown in Table 1 where the Principle of Least Action correctly selects for $^{163}_{66}\text{Dy}$, but not along the normal decay pathway. Instead the Principle of Least Action selects for $^{167}_{69}\text{Er}$ with a mass change of +0.0775065 amu. This is followed by alpha decay to $^{163}_{66}\text{Dy}$, still within the domain of reversible thermodynamics. The energy change drops accordingly to +0.0767937 amu. The overall mass change which normally manifests as gamma absorption, occurs instead as Mössbauer resonance; part of the far-from-equilibrium black body spectra..

I have chosen to call this mode of nuclear decay, where no intermediate radioactive products occur, and where half-life time delays are nonexistent, sigma-decay.

We are finally ready to look at the issue of excess heat generated in Miley's experiment. The LANP reversibility constraint requires that the core process be adiabatic. Therefore, we need to explore the limits of that process to identify the step at which it crosses over the line into the domain of irreversibility.

Because there are both exothermal (– mass change) and endothermal (+ mass change) reactions occurring, the excess heat is probably a net heat measure, and most probably has its origin in the circumstance where the far-from-equilibrium

spectrum is already filled at the gamma emission's frequency, and the energy must instead flow into the spectra's mass domain. There it enters the domain of irreversible processes, and results in an increase in T_m . The transfer function that re-distributes the gamma energy is theorized to be Eq. (2). Furthermore, experiments where no excess heat is observed could be either: (1) dominated by endothermal reactions, or (2) have a net zero heat production. The electrodes from these 'failed' experiments need to be checked for transmutation products. It is entirely possible that these experiments were successful in some way other than excess heat production.

5. Discussion

The LANP theory is unique in its ability to describe many of the unexplained phenomena occurring in a F&P electrolytic cell including:

- (1) A mechanism for loading energy into the metal hydride lattice,
- (2) A mechanism for storing that energy until ignition,
- (3) A theoretical basis for the fusion temperature requirement and how it is masked,
- (4) A mechanism for selecting products that do and do not occur,
- (5) An explanation for the absence of radioactivity.

The theory also has appeal in that it is not nickel specific, or even metal lattice specific, and it provides a plausible mechanism for the solar temperatures that thermonuclear fusion is known to require. LANP is a very hot process.

The mechanism that causes excess heat may require more detailed work, particularly with the nuclear event sequence that fills the far-from equilibrium spectra, and the meaning of equation [2], including its more rigorous derivation. Nevertheless, the model demands additional study and experimental work. It answers too many questions to be dismissed.

On the other hand, theoreticians and experimentalists in the field should contain their exuberance for this, or any other promising model. This field is simply too controversial to allow missteps, or premature dialog with the non-scientific community.

Places where LANP departs from current theory, and more importantly, from common sense, need immediate study. For example, is it even plausible that all of the intermediate radioactive decay steps, and half-life constraints of σ -decay can be bypassed by LANP. The absence of any radiation signature in F&P cells, and the observed transmutation products make that conclusion tantalizing. And yet, it is contrary to everything that we currently know about nuclear processes. The same is true of more fundamental aspects of the theory such as its claim of reversibility. This one feature of the theory is without precedent in modern science, and will be attacked vigorously in peer review. Perpetual motion machines, quite simply, are not supposed to exist. Even more implausible is the claim that stellar and supernova processes might occur within a laboratory device.

These claims are almost untenable, and yet they seem to constitute a cohesive theoretical framework that is consistent with the data. We should be very careful not to give LANP too much credibility at this point in its short life, and instead design a scientific plan to achieve rigorous experimental proof one way or the other.

Appendix A - The Tunneling Issue

The fundamental problem in cold fusion theory is overcoming the coulomb barrier between reacting nuclei. The barrier can be represented by the electro-static potential energy:

$$U_{\text{Coulomb}} = 2kZ_1Z_2e^2/l,$$

($Z_1 = 1$, $Z_2 = 28$)

where k is the Coulomb's constant, e the elementary charge, l the charge separation, and Z_1, Z_2 are the atomic numbers of the interacting nuclei. Overcoming this potential barrier for deuterium–deuterium fusion requires kinetic energies in the MeV range, essentially solar surface temperatures.

Parmenter and Lamb [11] showed how dual deuterons in a single potential well might achieve the required resonant energies in the presence of large numbers of conduction electrons which effectively masked the coulomb barrier. Subsequent investigators have proposed refinements to this resonant tunneling model, incorporating enhanced electron mass [12], resonant nuclear states [13], and calculated tunneling enhancements [14]. None of the tunneling theories put forward to date has proven sufficient to explain cold fusion experiments.

This issue is magnified in the current research because fusion reactions beyond the elementary four nucleon model are not only proposed, but presented without reference to the enormous coulomb barriers that they imply. For example, the $H + Ni$ and $Ni + Ni$ ($Z_1 = 1, Z_2 = 28$) Coulomb barriers are approximately 25 and 750 times greater, staggering energy barriers relative to the simple four nucleon problem. And yet, if the experimental results of Miley [15] and Mizuno [16] are to be believed, nature overcomes these incredible coulomb barriers in room temperature experiments every day.

The one remarkable characteristic of the reversible thermodynamic, framework employed by the LANP model, is the way that the time differentials, regardless of their mechanism, become identically zero. This occurs regardless of the order of the derivative (second order in the case of coulomb barrier repulsive force). Therefore, it is entirely possible that when we treat the cold fusion *process* as a reversible thermodynamic system, all of the repulsive coulomb barrier acceleration terms disappear from our model, and reactions that are possible at the operative radiation temperature, all become candidates for the reactor's next step. Possible reactions do not cascade randomly, but proceed stepwise in a systemized manner described entirely by the Principle of Least Action. One occurs. Then the next step occurs, and the next, and so on. This is the Least Action Nuclear Process. I discuss some of the fundamentals involved in [17], where I have included a calibration of my Theory of Heat; the larger research project that this paper is derived from. The LANP theory does not require tunneling. The coulomb repulsion terms a in $f_{\text{Coulomb}} = ma$ have all gone to zero.

Appendix B. The Gamma Conundrum

The LANP model differs from all other nuclear models in two important ways. First, it produces only stable nucleotides, and in fact, expected unstable isotopes and excited nuclear states *never* occur within the process. These are entropic quantities that are foreign to the reversible thermodynamic state, and cannot be produced within it. The only relevant quantities are the initial and final (Least Action) states.

Gamma energies are produced. For example, in Section 4, I refer to a fusion reaction: ${}^{58}_{28}\text{Ni} + {}^{107}_{47}\text{Ag} + {}^2_1\text{H}^+ \xrightarrow{\text{fusion}} {}^{162}_{66}\text{Dy}$ which normally results from six discrete beta decays and an alpha decay. Yet, no beta decay products are measured, nor are any of the intermediate unstable isotopes detected. The reversible thermodynamic process began with the three reactants, and produced one stable isotope and consumed a gamma photon ($0.07607937 \text{ amu} = 70.86489 \text{ MeV}$).

Secondly, although the LANP model produces these gamma energies, it liberates no gamma photons. Instead gamma quanta are theorized to be absorbed and emitted within the far-from-equilibrium blackbody spectra where these quanta are Mössbauer resonant between identical nuclei, and thus masked from observation beyond the limits of that absorption/emission process. In the circumstance where the far-from-equilibrium blackbody spectra has no vacancies to accommodate the gamma photon, its energy dissipates into the low energy spectra where it deteriorates to heat of motion, i.e. 'excess heat'.

Section 3 describes how Mössbauer resonant gamma energy alone defines the effective temperature within the LANP's metal lattice. For this model to evolve, it is a sufficient condition, that the lattice's *radiation temperature*, T_R , described by the Mössbauer resonant gamma field, achieve solar core temperatures.